An Active-Shunt Diverter for On-load Tap Changers

Daniel J. Rogers, *Member, IEEE*, and Tim C. Green, *Senior Member, IEEE*

***Abstract*—This paper presents a new hybrid diverter design for on-load tap changers. The design uses "active-shunt" current diversion principles. At its core, the design employs a low-voltage high-current switch-mode amplifier to divert current out of the mechanical contacts and into a pair of anti-parallel thyristors. Commutation between transformer taps may then be performed by the thyristors. The amplifier and thyristors are placed outside the normal load current path and only conduct during a tap change, producing efficiency savings and improving robustness when compared to previous hybrid on-load tap changer implementations. An amplifier control loop that autonomously produces zero-current conditions at switch opening and zero-voltage conditions at switch closure is demonstrated. Experimental results investigating the wear characteristics of contacts operated under the new hybrid diverter are presented, along with comparison results from a passive-type switching scheme. Contact lifetime of more than 25 million operations is demonstrated under the new scheme.**

***Index Terms*—Arc discharges, closed-loop systems, contacts, power distribution, power electronics, power grids, smart grids, sparks, transformers, voltage control.**

I. Introduction

THE distribution network of the future faces very significant challenges in accommodating the expected degree of penetration of distributed renewable energy and electric-vehicle charging. It has been recognized that export of power from photovoltaic (PV) systems causes voltage rise in distribution networks and that strategies to combat this are needed [1], [2]. The manipulation of reactive power by PV systems and curtailment of power export are options [3], but clearly curtailment is economically unattractive and reactive power becomes less effective as the X/R ratio reduces in low-voltage (LV) networks. It is also known that PV power export is subject to rapid fluctuations of power production due to the passing of cloud shadows. Studies [4] have shown that a considerable amount of smoothing of the output is obtained between even adjacent systems in the 10-s time frame but over minutes, the variations are correlated and large aggregate fluctuations occur. It was found that a separation of 50 km was required for changes over 30 min to be uncorrelated.

Manuscript received September 26, 2011; revised April 04, 2012 and June 02, 2012; accepted January 21, 2013. Date of publication March 13, 2013; date of current version March 21, 2013. This work was funded by a UK EPSRC Doctoral Training Award and was conducted partly within the Supergen FlexNet Program. Paper no. TPWRD-00827-2011.

D. J. Rogers is with the Institute of Energy, School of Engineering, Cardiff University, Cardiff CF24 3AA, U.K. (e-mail: RogersDJ@cardiff.ac.uk).

T. C. Green is with the Electrical and Electronic Engineering Department, Imperial College London, London SW7 2AZ, U.K. (e-mail: t.green@imperial.ac.uk).

Color versions of one or more of the figures in this paper are available online at http://ieeexplore.ieee.org.

Digital Object Identifier 10.1109/TPWRD.2013.2243171

Existing distribution network voltage-control mechanisms, which rely on on-load tap-changers (OLTCs), were designed for the slow adjustment of gradual demand changes over a daily cycle. It is possible to provide fast and accurate voltage control using "electronic transformers" (for instance, [5]), but as yet, these devices are not competitive in terms of power losses, capital cost, or footprint with conventional OLTC-equipped transformers. The duty of an OLTC providing voltage control on feeders rich in PV and EV could be very high. As an illustration, suppose that the OLTC reacted at 5-min intervals and that on most occasions, only a single-tap increment was needed but on 10% of occasions, 5-tap increments were required due to either shadowing of PV or correlated EV charging. It is possible that 400 tap changes per day may be seen, leading to 150 000 tap operations per year and 6 million tap operations over a 40-year life. OLTC manufacturers are now offering devices based on vacuum switches rather than more traditional contacts in oil [6], [7]. These are quoted as having a service interval of 300 000 operations and a lifetime of 2 million operations [8]. For widespread use in distribution substations of the future, much greater service intervals are needed and it is probably necessary to reduce the physical volume of the OLTC diverter element to allow retrofit to existing substations. This observation provided the motivation for the work to be described here which seeks to achieve wearless operation of OLTC contacts by providing zero-current opening and zero-voltage closing with a shunt-connected active element.

While yet to see significant commercial uptake, several OLTC designs containing semiconductor devices have been presented in the literature in the past 50 years. These designs seek to dramatically reduce the degree of arcing occurring at the mechanical diverter contacts. Although some designs directly replace the mechanical contacts with semiconductor devices (e.g., [9] and [10]), it is often suggested that mechanical switching elements should not be eliminated entirely. Hybrid (or "semiconductor-assisted") OLTC designs are presented where semiconductor devices are used to perform current interruption/commutation but mechanical switching elements are retained for use during steady-state operation. In this way, the strengths of both devices are exploited: semiconductor devices provide wearless commutation capability during a tap change operation while mechanical contacts provide very low on-state resistance and correspondingly small power loss during steady-state (fixed tap) operation. The method by which the current transfer between the mechanical switch and semiconductor device is achieved during the commutation process leads to a natural separation of the hybrid diverter designs into three categories, as shown in Fig. 1.

The objective of this paper is to explore in detail the circuit of 1(c) (the active-shunt diverter) in comparison with those of 1(a) and (b) (the passive and active-series diverters). The active

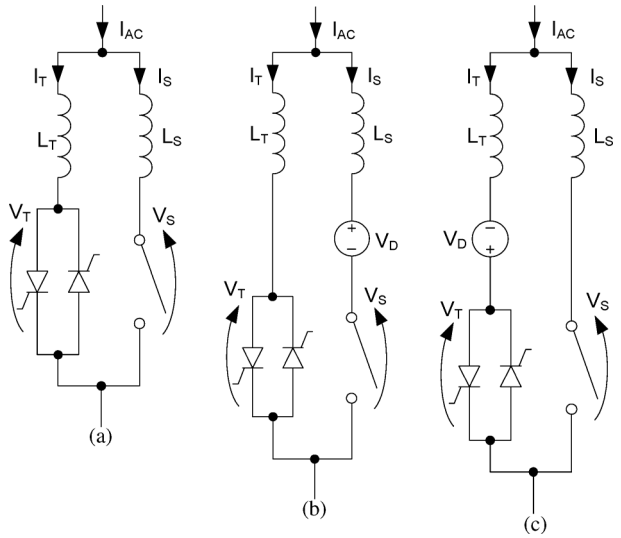

Fig. 1. Classification of hybrid OLTC schemes. (a) Passive. (b) Active series. (c) Active shunt.

shunt circuit was introduced in [11] and [12], and experimental results used to demonstrate its effectiveness. In this paper, the tap sequence and operation of the active element are described in detail (with an improved control configuration over [11]), a discussion of arc energy and its implication for contact wear is given, and a full comparison of the passive and active configurations is undertaken. To begin, these three diverter configurations will be described.

A. Passive Type

The passive-type hybrid OLTC relies on the process of mechanical contact separation to drive current into an alternate path. Typically, the alternate path contains a pair of antiparallel thyristors (either line commutated or gate turn-off type). An example passive scheme is that of [13] where the increasing voltage drop across an opening mechanical contact is used to trigger a thyristor into conduction via a pulse transformer, providing an alternate current path at some instant after the moment of contact separation. The principle drawback of passive-type schemes is that arcing at the switch contacts may never be entirely eliminated. Fig. 1(a) illustrates a conceptual circuit that includes two parasitic inductances (labelled L_S and L_T) that inevitably occur in any practical circuit implementation. Upon opening of the switch and assuming the forward thyristor is triggered into conduction beforehand, these inductances act to limit the rate of transfer of load current $(I_{\rm AC})$ between the switch (I_S) and the thyristor (I_T) paths.

B. Active Series Type

Active-series hybrid OLTC designs are characterized by the placement of an opposing voltage source (V_D) in series with the mechanical switch. The activation of this voltage source causes current to transfer out of the switch path and into an alternative path containing semiconductor devices, such as thyristors. [See Fig. 1(b).] This is achieved *without* opening the switch under load: after the current has been fully transferred, the switch may be opened under a condition of zero current, eliminating contact arcing. An example of an active-series design is found in [14] where the series voltage source is called the "auxiliary current diverter."

C. Active Shunt Type

In the active-shunt configuration illustrated in Fig. 1(c), the voltage source is placed in the thyristor diversion path instead of the switch path. The source is connected such that it acts to cancel the thyristor forward voltage and is controlled to drive a current equal to the load current through the alternate path $(I_T = I_{\rm AC})$. In this case, the current in the switch will be zero, and the arcless operation of the switch is ensured. The main advantage of the active shunt scheme over the active series scheme is that no additional device must be inserted in series with the steady-state load current path (i.e., the switch path). Thus, no additional steady-state power loss is incurred and, for the majority of time, no semiconductor device is exposed to the load current and, hence, to possible fault currents. Only during current diversion (i.e., during a tap change operation) is the active device required to conduct the load current. The disadvantage of the active shunt design is that active control of the voltage source is required to provide sustained zero-current conditions in the switch.

In a well-designed active system, the current at the switch opening will be very low, governed by leakage current through the voltage source (for the series design) or by control-loop errors (for the shunt design). Therefore, switch contacts operated under either scheme may be expected to experience low wear rates and deliver very long service lifetimes. The primary operational difference lies in the fact that the shunt design does not experience the steady-state power loss associated with the continually conducting voltage source of the series design.

In the active-series and active-shunt circuits, the voltage source, while required to conduct the full-load current, is only required to sustain a voltage approximately equal to that of the conducting thyristor in order to cause current diversion. For LV and MV OLTC systems, single-junction thyristors provide ample voltage blocking capability and the required source voltage will less than 10 V.

II. Arcless OLTC Based on the Active Shunt Principle

Fig. 2 shows the high-level circuit implementation and the operating steps of a new OLTC diverter based upon the active shunt principle. Similar to most OLTCs, the design can be separated into a selector section and a diverter section. The selector section is capable of connecting any odd-numbered tap to the left "leg," and any even-numbered tap to the right leg. The system operates by transferring the load current between legs; each transition allows a different tap to be selected as long as the new tap is on the opposite leg. The selector contacts are never required to make or break current; this function is handled by the diverter section. The diverter section of the new OLTC design consists of two mechanical switches (S_L and S_R), two sets of antiparallel thyristors [T_{L+}, T_{L-}] and [T_{R+}, T_{R-}]), and a "controlled source" which may be operated such that it behaves

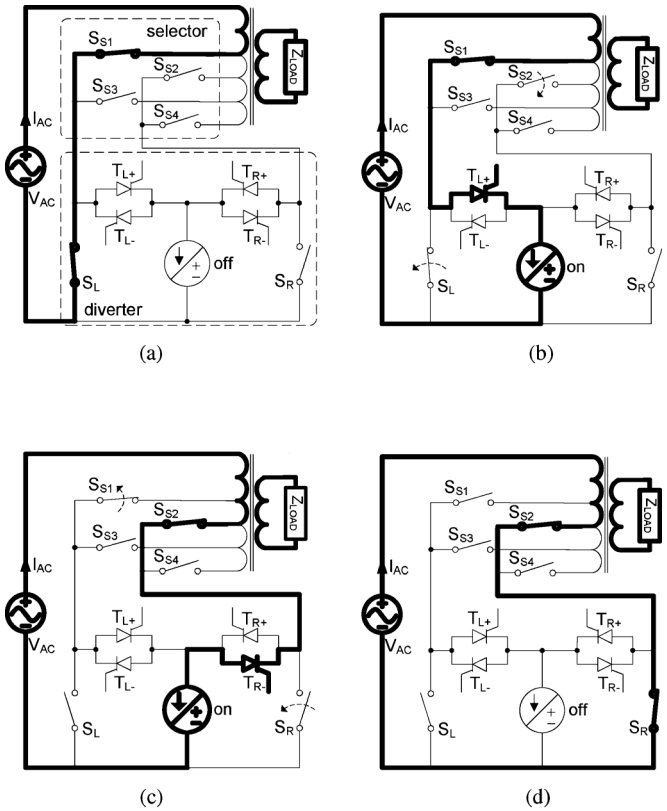

Fig. 2. Current paths in the active shunt OLTC design when performing a single tap-up operation from tap 1 to tap 2. See Fig. 3 for time references. A finer-grained breakdown of the tap-change sequence is given in [11]. (a) $t < t_C$. Steady-state operation on tap 1. Controlled source off. (b) $t_C < t < t_F$. S_L opens under a condition of zero current. S_{S2} begins closing in preparation for operation on tap 2. (c) $t_F < t < t_l$. S_L open. S_R closes under a condition of zero voltage. S_{S1} begins opening in preparation for operation on tap 2. (d) $t_l < t$. Steady-state operation on tap 2. S_R is closed and the controlled source is off.

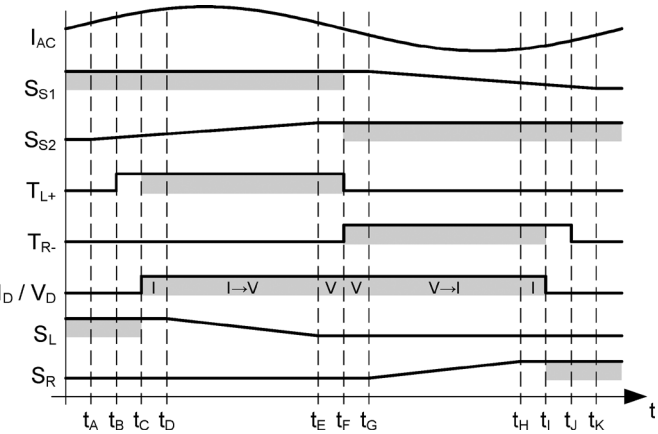

Fig. 3. Idealized timing diagram for a tap change performed over one cycle of the load current. A high level for S_{S1}, S_{S2}, S_L, S_R indicates the corresponding switch is closed, a low level that the switch is open, intermediate values represent a switch that is changing state and is neither open nor closed. A high level for T_{L+}, T_{L-} indicates that trigger current is applied. A high level for I_D/V_D indicates that the controlled source is operating, the I or V entry denotes current or voltage source mode, respectively. Shaded regions indicate device conduction.

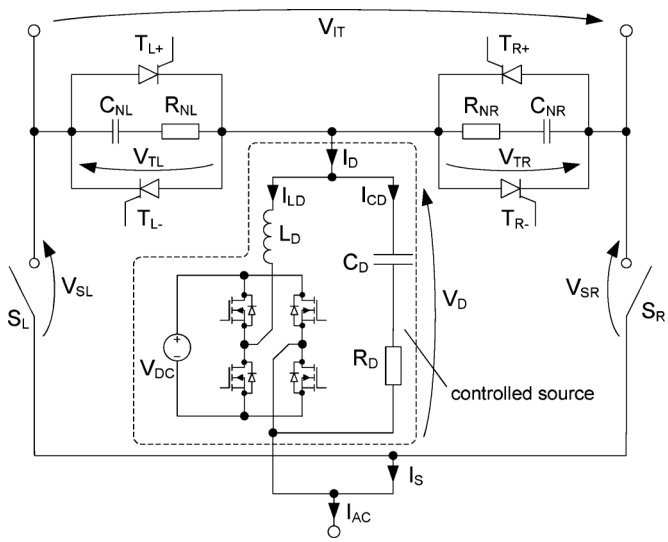

Fig. 4. Active shunt OLTC diverter circuit.

as either a current source or a voltage source as required (hence, it is illustrated as both in Fig. 2).

The fundamental task of the diverter sub-circuit in the new design is identical to that of the diverter in the classic, purely mechanical OLTC: to transfer the load current between the switches without interruption. However, an additional task of the new diverter is to ensure zero-current or zero-voltage conditions are maintained during switch operation. While either the left or the right switch is closed, a condition of zero current may be created by triggering the corresponding thyristor pair into conduction and operating the controlled source in current mode such that it produces a current equal to the load current. In this case, the load current flows through the controlled source leaving zero residual current in the switch. Similarly, during a period in which either switch is open, a condition of zero voltage may be created by triggering the thyristor pair into conduction and operating the controlled source in voltage mode such that it produces a voltage that exactly counterbalances that of the conducting thyristor. In this case, the sum of voltages in the loop around the switch is zero and there is zero potential across the switch contacts.

Commutation between left and right legs of the diverter is performed at the zero-crossing of the load current. The trigger signal for the outgoing thyristor is removed so that it transitions to the blocking state at the zero-crossing, at which point the reverse-facing thyristor on the opposing leg is triggered. Fig. 3 shows the timing of the transitions between steps.

A. Diverter Circuit and the Controlled Source

Fig. 4 shows one possible device-level implementation of the hybrid-shunt diverter. The controlled source is switch mode in nature, employing four low-voltage, high-current MOSFET devices in an H-bridge configuration. The inductor L_D is included so that current-source behavior may be produced through suitable closed-loop control of the H-bridge duty cycle when one of the two switches (S_L or S_R) is closed. C_D and R_D are present to define the voltage V_D when both switches are open. RC snubbers are placed across both thyristor pairs to aid commutation between diverter legs at the load current zero crossing.

The H-bridge must be capable of driving a sinusoidal current equal to the load current through the inductor $L_D(I_{LD})$. The maximum average value of V_A is equal to the supply voltage $V_{\rm DC}$. Given a worst case thyristor forward voltage drop of $V_{T(\max)}$ and assuming negligible parasitic series resistances the maximum allowable size of L_D is given by

$$L_{D(\max)} = \frac{V_{\rm DC} - V_{T(\max)}}{\omega_0 I_0} \tag{1}$$

where I_0 is the peak load current and ω_0 is the line angular frequency. For cost and size reasons it is desirable to keep L_D and $V_{\rm DC}$ small. However, the design must be tolerant of variations in the inductor value, as well as parasitic circuit resistances that will tend to reduce the achievable rate of change of current through the inductor. Therefore reasonable choices are $V_{\rm DC} = 2V_{T(\max)}$ and $L_D = L_{D(\max)}/2$. For distribution network applications $V_{\rm DC}$ and L_D will lie in the region of 7 V and 50 μH, respectively. C_D and R_D are less critical in terms of their sizing, but they should be chosen such that they provide good attenuation of the ripple current produced by the H-bridge. For distribution network applications, C_D and R_D will be in the region of 100 μF and 1 Ω, respectively.

The use of MOSFETs in an OLTC represents an interesting third level of hybridization over that seen in previous systems. Mechanical switches are exploited for their low conduction losses and high robustness, thyristors are used for their high-voltage high-current wearless commutation capabilities, and MOSFET devices are included to provide a highly controllable, low-voltage high-current amplifier device in the form of the controlled source.

B. Commutation Between Diverter Legs

Current commutation between diverter legs occurs around the zero-crossing of the line current (e.g., between Figs. 2(c) and (d)). If the commutation process is not handled carefully an inter-tap short-circuit may be established should the incoming thyristor be triggered before the outgoing thyristor has fully recovered its blocking capability. For this to occur, the inter-tap voltage $V_{\rm IT}$ must be of a magnitude and direction that will forward bias the incoming and outgoing thyristors. This scenario is encountered in exactly half of all possible commutation events. A commutation event is described by the following four variables: tap direction (up or down), commutation direction (left-to-right or right-to-left), current zero-crossing direction (positive-to-negative or negative-to-positive) and power factor (load current leading or lagging the inter-tap voltage). An exhaustive list of potential short-circuit cases may be generated by considering all possible combinations of the these variables. In order to avoid the introduction of an inter-tap short-circuit, the triggering of the incoming thyristor is delayed for a short time after the current zero-crossing in order to guarantee that the outgoing thyristor has fully recovered its forward blocking capability. In this period the load current must flow in the snubber components, the resulting snubber voltage should be limited by appropriate selection of the snubber components ($C_{\rm NL}$, $R_{\rm NL}$, $C_{\rm NR}$ and $R_{\rm NR}$).

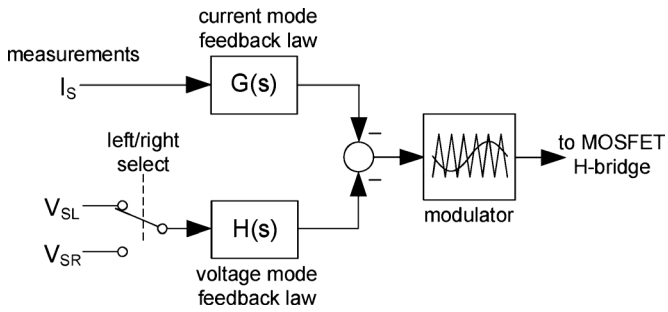

Fig. 5. Feedback law for zero-current, zero-voltage operation of the diverter circuit of Fig. 4.

C. A Diverter Feedback Law

Fig. 5 shows one possible feedback law arrangement that is capable of producing the desired zero-current zero-voltage conditions. The system requires measurements of the sum of the switch currents (I_S), and both switch voltages ($V_{\rm SL}$ and $V_{\rm SR}$). The diverter circuit exhibits different behavior depending on whether one of the switches (S_L or S_R) is closed or both are open (the switches may never be closed at the same time as this would introduce an inter-tap short circuit). This implies that two different plant models are required when designing the compensators $G(s)$ and $H(s)$, one that represents the circuit with one switch in the closed state and one that represents the circuit with both switches in the open state. Simplified control loop models for both states are illustrated in Fig. 6. While operating with a switch closed, the corresponding voltage measurement across that switch is, by definition, zero; hence, the output of the $H(s)$ block is also zero and $G(s)$ acts to drive I_S to zero. This is called the *current mode*. Similarly, when both switches are open, I_S is, by definition, zero and, therefore, the output of the $G(s)$ block is zero; $H(s)$ acts to drive either $V_{\rm SL}$ or $V_{\rm SR}$ to zero depending on the position of the selector switch. This is called the *voltage mode*. The effect of the (non-linear) thyristor forward voltage ($V_{\rm TL}$ or $V_{\rm TR}$ in Fig. 4) is modelled by the disturbance input $V_{\rm dis}$, this voltage may be considered almost independent of the control loop action during normal operation due to the weak dependence of thyristor voltage on forward current. While in current mode, the rapid reversal of this voltage at the current zero-crossing acts to drive a current impulse through C_D ($I_{\rm CD}$ in Fig. 4) limited in magnitude by R_D. This current disturbance is modelled by the input $I_{\rm dis}$ in Fig. 6(a).

It is important to note that the feedback law of Fig. 5 is *fixed* for both circuit states: it is *not* designed as two separate feedback systems which must be "switched in" depending on the circuit state. The feedback law requires no external signalling to identify the moment at which the switch contacts close or separate; it transitions autonomously between current and voltage modes as the switches are operated.

Given sensor and amplifier transfer functions that may be approximated as a first-order low-pass filter with a cutoff frequency in the region of 50 kHz, good results have been achieved for the first-order feedback law transfer functions given in Fig. 6 ($G(s)$ is a first-order lead and $H(s)$ is a first order lag.) The parameters g, ω_g,, h, and ω_h depend on the values of L_D, C_D, and

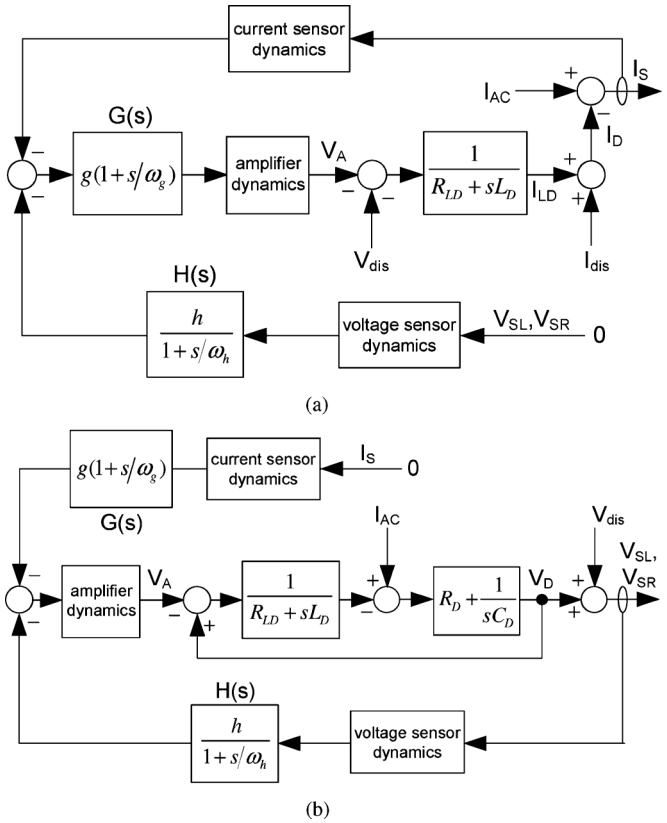

Fig. 6. Simplified control loop representations of the diverter circuit of Fig. 4 operating under the feedback law of Fig. 5. R_{LD} is the parasitic resistance of L_D (not shown in Fig. 4). (a) Either switch closed (current mode). (b) Both switches open (voltage mode).

R_D. Experience suggests that a residual switch current (i.e., current remaining flowing in a closed switch despite action of the feedback law in current mode) of less than 0.5% of the nominal load current is readily achievable. Residual switch voltages (i.e., voltage remaining across an open switch despite action of the feedback law in voltage mode) are typically in the region of 100 mV. In most practical switch-mode implementations, such as those in Fig. 4, the residual switch current and voltage is dominated by switch-mode ripple as opposed to the error resulting from finite gain of the feedback law.

III. Experimental Comparison of Passive and Active-Shunt Contact Protection

Active-type OLTC schemes (whether they be series or shunt designs) may theoretically offer completely arcless operation of their mechanical contacts. Thus it may be expected that arc induced wear mechanisms will be entirely eliminated and secondary wear mechanisms, such as mechanical wear, will become dominant. However, any *practical* implementation of these systems cannot be expected to achieve absolute zero-current, zero-voltage conditions, due to (in the active-shunt case) a combination of measurement error, finite feedback gain and switch-mode ripple components. Some residual current will remain flowing in the switch at the moment of contact separation and therefore a small degree of arcing should be expected. Passive-type schemes by their very nature must sustain a degree of arcing to facilitate current transfer into the alternate path.

The following experimental results demonstrate that a practical active-shunt design may nevertheless provide greatly reduced wear characteristics when compared to a passive-type circuit: contact wear rates less than one fifth that of a highly-optimised passive-type circuit were obtained and are illustrated in Fig. 7. Although not tested explicitly, the active-shunt contact wear results should be considered to be an indication of what might be achieved under an appropriately designed active-series scheme due to the similar current profiles experienced during switch opening. The experimental apparatus used to obtain the active-shunt results was designed for a load current of 100 $\mathrm{A_{pk}}$ and an inter-tap voltage of up to 300 $\mathrm{V_{pk}}$, ratings that roughly correspond to a 1.3-MVA 11-kV primary-side OLTC. Details of the circuit construction and the test environment used to produce the load current and intertap voltages are described in a previous paper by the authors [12].

A. Arc Energy as an Indicator of Wear

The contact wear caused in a particular opening event may be expected to be strongly determined by the current at contact separation: large currents will produce more intense arcs and damage the contacts to a greater degree. However, the initial arc current does not capture the length of time over which the arc may be sustained. For example, for a switch protected by the passive diverter scheme of Fig. 1(a), the initial arc current is equal to that of an "unprotected" switch (i.e., a switch operated in a circuit where no alternate current path exists). However, in the case of the protected switch, the current rapidly diverts into the parallel path, and the arc is extinguished rapidly.

It is proposed that the *energy* dissipated in the arc will be a better indicator of arc induced contact wear than arc current alone. It is assumed that greater arc energy will translate into greater contact wear but that the duration of the arc is less important. For a particular switching event, n, the arc energy for that event is defined as

$$E_n = \int_{t_o}^{t_e} V_a(t) I_a(t) \cdot \mathrm{d}t. \tag{2}$$

$V_a(t)$ is the arc voltage (i.e., the voltage across the switch contacts during the arcing process). $I_a(t)$ is the arc current (equal to the switch path current). The product $V_a I_a$ is always positive, that is, the arc is dissipative and the arc voltage sign depends on the arc current direction. t_o is the time at which the switch is opened and t_e is the time at which the arc extinguishes. The extinction time depends on the evolution of the arc over time which in turn is dictated by the electrical circuit of which the switch is a part. The arc may be expected to extinguish and form an open circuit when the current through it drops to near-zero. The *total arc energy* over N switching operations may calculated as

$$E_{\mathrm{tot}} = \sum_{n=1}^{N} E_n. \tag{3}$$

It is proposed that any particular contact design will have associated with it an end-of-life E_{tot} at which it will considered to be too worn for reliable service and must be replaced. Under this assumption a set of contacts dissipating half the energy

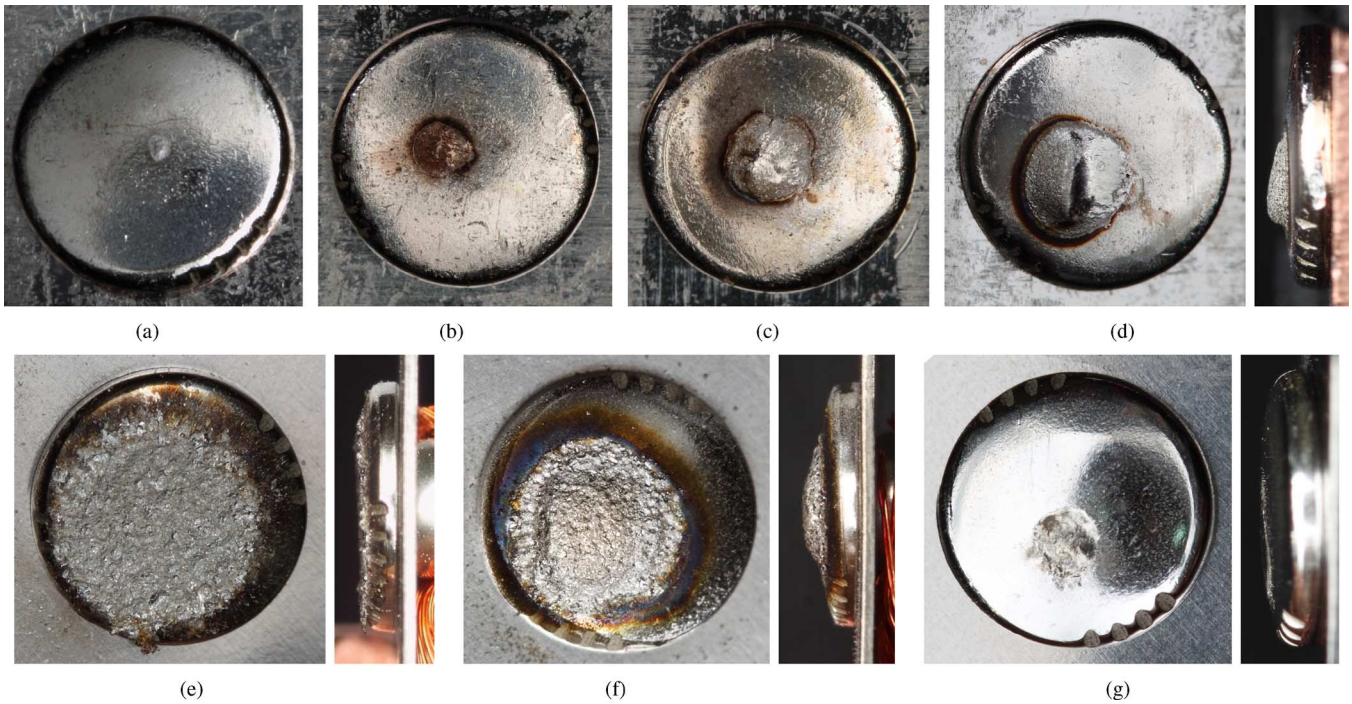

Fig. 7. Front and side photographs of sample contacts operated under a variety of conditions (number of operations are given in brackets; all contacts operated with a sinusoidal load current of 100 A peak except for (a) and (g); contact diameter is 3.60 mm). Note that the opposing contacts show similar wear patterns (not pictured): for (e) and (g), similar material loss was evident; for (d) and (f), a corresponding crater was present. All contacts are from a high-current automotive-type relay [15]. The contact material is $AgNi_{0.15}$ and the contact standoff distance is 0.8 mm. (a) Unused (0), (b) active shunt (4.04×10^6), (c) active shunt (1.10×10^7), (d) active shunt (2.56×10^7), (e) passive (1.88×10^5), (f) passive zero-crossing (5.17×10^6), (g) mechanical only (6.55×10^7).

per switching event may be expected to last for twice as many switching operations, that is, the average energy dissipated by the contacts ($E_{\rm av} = E_{\rm tot}/N$) may be used as an indicator of switch wear *rate*. Clearly this simple analysis does not take into account other wear processes (e.g., mechanical abrasion). However, during the course of this study the arc-energy method was observed to correlate well with the visual appearance of worn contacts and so $E_{\rm tot}$ calculations are presented to provide a secondary basis for the comparison of different diverter schemes beyond the subjective visual comparison allowed by Fig. 7.

A calculation of arc energy is now presented subject to three simplifying assumptions. Firstly, the current transfer process is assumed to occur in a time much shorter than the period of the load current, such that the load current may be approximated as remaining constant during the transfer process. Secondly, the arc is assumed to never 're-strike' after it has extinguished. Thirdly, both the arc voltage and the thyristor voltage are taken to be constant during the transfer process. An arc voltage of $V_a = 12$ V and a thyristor voltage of $V_T = 7.3$ V were found to be good approximations to the actual voltages observed during the experimental phase (note that the thyristor voltage is relatively high due to the device forward recovery characteristic, see [12] for an illustration of arc voltage/current waveforms). If the switch is opened at time t_o the arc current is described by

$$I_a(t) = I_s(t_o) - \frac{V_a - V_T}{L_S + L_T}(t - t_o) \tag{4}$$

where $I_s(t_o)$ is the current flowing in the switch at the moment of opening. In the passive diverter scheme this current is equal to the OLTC load current at this instant. In the active diverter schemes it is equal to the residual current remaining in the switch after action of the controlled source. Assuming an arc voltage such that $V_a > V_T$, the arc extinction time is given by the solution of (4) ($I_a(t_e) = 0$). The arc energy is then given by

$$E_a = \int_{t_o}^{t_e} V_a I_a(t) \cdot {\rm d}t = \frac{V_a(L_S + L_T)}{2(V_a - V_T)}(I_s(t_o))^2. \tag{5}$$

B. Average Arc Energy in the Passive-Type Comparison Circuit

The passive-type circuit considered here is functionally that of Fig. 1(a). The parasitic loop inductance $(L_S + L_T)$ was minimized by keeping the switch-thyristor wiring short (experimentally found to be 260 nH). Two passive-type tests were conducted: the first was performed such that the switch opening times were distributed randomly throughout the line cycle. The second test was performed so that switching was constrained to occur in a well-defined period around the zero-crossing of the load current; in this case, the residual switch current is much smaller than the peak load current and, therefore, the average arc energy experienced by the switch is much lower.

The passive-type test is characterized by a sinusoidal switch current of $I_s(t_o) = I_0 \sin(\omega_0 t_o)$. If t_o is distributed uniformly across a region $2m\pi/\omega_0$ centred around the current zero

crossing, the average arc energy per switching operation (averaged over a large number of operations) may be calculated by

$$E_{\rm av} = \frac{\omega_0}{2m\pi}\int_{-m\pi/\omega_0}^{m\pi/\omega_0} E_a(t_o)\cdot {\rm d}t_o, \\ = I_0^2\left(1-\frac{\sin(2m\pi)}{2m\pi}\right)\frac{V_a(L_S+L_T)}{4(V_a-V_T)}. \quad (6)$$

For the contact of Fig. 7(e), $m = 1$ (i.e., switching operations may occur at any point in the load current cycle). For the contact of Fig. 7(f), $m = 0.05$ (i.e., switching operations are constrained to fall within 1 ms of the load current zero crossing, assuming a line frequency of 50 Hz). For a peak load current of $I_0 = 100$ A, the average arc energies are 1.6 mJ and 26 μJ, respectively.

C. Average Arc Energy in the Active Shunt Diverter Circuit

An experimental active shunt diverter was constructed based on the circuit and feedback law structures presented in Figs. 4 and 5, respectively [12]. For the test environment used in this study, the residual switch current at the opening in the active-shunt scheme may be characterized by an error current I_e (present due to control-loop error) plus a triangular ripple component of magnitude ΔI (present due to the switch-mode nature of the controlled source) as follows:

$$I_s(t_o) = I_e + \Delta I\Lambda(ft_o) \quad (7)$$

where $\Lambda(x)$ is the triangle-wave function of period and amplitude 1 and where $f = 1/T$ is the ripple current frequency. Since the triangle-wave period was observed to be large compared to the arcing time (typically $t_{\rm arc} \approx 0.1T \approx 1\mu$s), (5) is assumed to provide a reasonable approximation of arc energy. It is further assumed that the opening time is uncorrelated with the ripple current waveform (i.e., switch opening is randomly distributed across the ripple current waveform). Under these conditions, the average arc energy per switching operation (averaged over a large number of operations) may be calculated in a similar manner to (6) by

$$E_{\rm av} = \frac{1}{T}\int^{T} E_a(t_o)\cdot {\rm d}t_o \\ = \left(3I_e^2+\Delta I^2\right)\frac{V_a(L_S+L_T)}{6(V_a-V_T)}. \quad (8)$$

Experimental observations give $I_e = 1$ A and $\Delta I = 1.5$ A. $L_S + L_T$ for the hybrid diverter is estimated at 1 μH due to the longer wiring path when compared to the passive-type circuit. In this case, and using the values for arc and thyristor voltages given previously, $E_{\rm av} = 5.0$ μJ.

D. Active Shunt Diverter Contacts

The hybrid diverter contacts of Figs. 7(b)–(d) demonstrate wear levels that increase with the number of operations. After over 25 million operations have been performed a clear pip-and-crater formation is visible (all contacts were fully functional at the end of the tests, despite pip-and-crater formation). This number of operations corresponds to over 1700 tap changes per day over a 40-year lifespan allowing, for example, minute-by-minute single-tap adjustment of the OLTC position.

TABLE I
AVERAGE AND TOTAL ARC ENERGIES FOR THE CONTACTS OF FIG. 7

Test type	Fig.	$E_{\rm av}$	Operations	$E_{\rm tot}$
Active diverter	7(b)	5.0 μJ	4,038,229	20 J
Active diverter	7(c)	5.0 μJ	11,048,643	55 J
Active diverter	7(d)	5.0 μJ	25,562,754	130 J
Passive	7(e)	1.6 mJ	187,822	300 J
Passive (zero cross)	7(f)	26 μJ	5,170,096	140 J

Pip-and-crater formation is a commonly observed phenomenon in contacts of this type operating at relatively low currents [16], [17]. It is clear that very little material loss has occurred and that pip-and-crater formation is very slow, suggesting that the potential lifetime number of operations for a contact used under the hybrid diverter could be exceptionally high, perhaps greater than 100 million should the standoff distance be increased significantly so that pip formation does not impact switch breakdown voltage. It is possible that other mechanical issues (e.g., fatigue) would become apparent before contact erosion caused switch failure.

E. Passive Circuit Contacts

The passively protected contact of Fig. 7(e) shows a complete loss of the contact surface rather than a redistribution of material as seen under the active diverter contacts. Material was observed to deposit on the inside of the switch housing (see [12]), confirming that material loss was occurring. The zero-crossing switched passive contact of Fig. 7(f) shows similar pip-and-crater formation as that of the active shunt diverter contacts. Note that while providing low contact wear rates roughly comparable to that achieved under the active diverter, it is posited that the operating method employed to generate the results of Fig. 7(f) is not feasible for practical OLTC applications due to the precise timing and mechanical tolerances required for reliable zero-crossing operation.

F. Mechanically Operated Contacts

Fig. 7(g) shows a contact that has performed more than 65 million operations with no electrical load. The number of operations is well beyond the mechanical lifetime stated by the manufacturer. Some mechanical flattening is evident in the front and side views, although the degree of wear is very small.

G. Correlation Between Contact Wear and Total Arc Energy

Table I summarizes the average and total arc energies for the contacts of Fig. 7 that were subject to an electrical load. The calculated total arc energies correlate well with the general visual appearance of the contacts: high total energies correspond to greater contact wear and vice-versa. It is clear that at least two quite different wear mechanisms exist depending on the average arc energy experienced. In the passive case of Fig. 7(e), material is *lost* from the contacts, whereas for both the active diverter and the passive zero-crossing switched contacts, it appears as though material is merely *redistributed* (although some small loss of material cannot be ruled out). Note that the passive contact experiences between 60 and 300 times the average arc energy of the other electrically loaded contacts; thus, it is reasonable to expect that different physical processes may be active in this case. More energetic arcing may allow material to

be forcibly ejected from the contact gap. It may be stated that roughly similar contact material volumes are affected (i.e., appear worn) in Figs. 7(d) and (f), despite a factor of five difference in the average arc energy experienced by each. However, the wear *rate* is very much lower in the case of the active-diverter contact; perhaps lower than might be expected considering the calculated arc energies (both contacts have experienced similar E_{tot}). Furthermore, the appearance of the pip formations are significantly different, with the active diverter producing much finer patterning of the surface of the pip with steeper sides and smaller footprint area. Interestingly, pip-and-crater formation occurs despite the fact that the contacts were operated under a nominally ac circuit with no large inherent bias as a result of current direction within the circuit. For the contacts of Fig. 7, the bias was of the order of 100 mA (determined by the offset performance of the current sensor and control loop circuitry). It is generally reported that $AgNi_{0.15}$ provides good resistance to pip-and-crater formation at the current levels employed in this study [17], [18]; thus, it is unlikely that a dramatic reduction in formation rate may be achieved by an alternate choice of contact material. However, the formation rates observed were very low such that for practically sized contacts suited to OLTC applications, it may be reasonably stated that arc-induced contact wear may be eliminated by the application of active shunt diverter principles.

IV. Conclusion

Active voltage control will become increasingly important as electrical networks develop. Especially on the distribution network, it is probable that greater voltage-control capability will be required as more intermittent generation is connected along already highly loaded feeders. In order to enable minute-by-minute use of OLTCs to control network feeder voltage, OLTC systems must be capable of performing tens of millions of operations over their installed lifetimes. Currently, this is beyond the reach of even advanced vacuum-interrupter-based systems. Hybrid OLTCs are a possible solution to this problem. Active shunt devices potentially offer excellent efficiency and electrical robustness due to the elimination of continuously conducting semiconductor devices in the load current path.

An active-shunt diverter circuit employing a third "level" of hybridisation, as well as a control loop design capable of sustaining zero-current zero-voltage conditions in either diverter switch was presented. The system ensures near-arcless operation of the diverter switches without the requirement for accurate knowledge and timing of the instant of contact separation or closure.

Experimental results comparing the wear rate of identical contacts used under passive and active shunt schemes were also presented. It was shown that the active shunt scheme may effectively reduce wear of the diverter switch contacts to a level where contact material loss (or transfer) is no longer a major limiting factor determining switch lifetime.

References

[1] R. Tonkoski, D. Turcotte, and T. H. M. El-Fouly, "Impact of high PV penetration on voltage profiles in residential neighborhoods," *IEEE Trans. Sustain. Energy*, vol. 3, no. 3, pp. 518–527, Jul. 2012.

[2] Y. Liu, J. Bebic, B. Kroposki, J. de Bedout, and W. Ren, "Distribution system voltage performance analysis for high-penetration PV," presented at the IEEE Energy 2030 Conf., Atlanta, GA, Nov. 2008.

[3] Y. Ueda, K. Kurokawa, T. Tanabe, K. Kitamura, and H. Sugihara, "Analysis results of output power loss due to the grid voltage rise in grid-connected photovoltaic power generation systems," *IEEE Trans. Ind. Electron.*, vol. 55, no. 7, pp. 2744–2751, Jul. 2008.

[4] A. Mills, M. Ahlstrom, M. Brower, A. Ellis, R. George, T. Hoff, B. Kroposki, C. Lenox, N. Miller, M. Milligan, J. Stein, and Y. H. Wan, "Dark shadows," *IEEE Power and Energy Mag.*, vol. 9, no. 3, pp. 33–41, May/Jun. 2011.

[5] S. Bifaretti, P. Zanchetta, A. Watson, L. Tarisciotti, and J. C. Clare, "Advanced power electronic conversion and control system for universal and flexible power management," *IEEE Trans. Smart Grid*, vol. 2, no. 2, pp. 231–243, Jun. 2011.

[6] C. Oates, A. Barlow, and V. Levi, "Tap changer for distributed power," presented at the Eur. Conf. Power Electron. Appl., Aalborg, Denmark, Sep. 2007.

[7] D. Dohnal and B. Kurth, "Vacuum switching, a well proven technology has found its way into resistance-type load tap changers," in *Proc. Transm. Distrib. Conf. Expo.*, 2001, vol. 1, pp. 161–165.

[8] Reinhausen Group, On-load tap-changer VACUTAP® VV technical data TD 203/04, Aug. 2010. [Online]. Available: http://www.reinhausen.com/

[9] E. Scheubeck, "Load Commutating System for Regulating Transformers," U.K. Patent, no. 1,126,840, Sep. 1968.

[10] J. Faiz and B. Siahkolah, "New solid-state onload tap-changers topology for distribution transformers," *IEEE Trans. Power Del.*, vol. 18, no. 1, pp. 136–141, Jan. 2003.

[11] D. J. Rogers and T. C. Green, "Zero-current zero-voltage switching for on-load tap changers," presented at the 5th IET Int. Conf. Power Electron., Mach. Drives, Brighton, U.K., Apr. 2010.

[12] D. J. Rogers and T. C. Green, "A hybrid diverter design for distribution level on-load tap changers," in *Proc. IEEE Energy Convers. Congr. Expo.*, Sep. 2010, pp. 1493–1500.

[13] G. Cooke and K. Williams, "New thyristor assisted diverter switch for on load transformer tap changers," in *Proc. Inst.Elect. Eng., B Elect. Power Appl.*, Nov. 1992, vol. 139, no. 6, pp. 507–511.

[14] R. Shuttleworth, X. Tian, C. Fan, and A. Power, "New tap changing scheme," in *Proc. Inst. Elect. Eng. Elect. Power Appl.*, Jan. 1996, vol. 143, no. 1, pp. 108–112.

[15] Tyco Electronics, Power relay F7/VF7 datasheet, Document ID V23134-X0000-A002, Aug. 2010. [Online]. Available: http://www.tycoelectronics.com/

[16] R. Holm, *Electric Contacts*, 4th ed. Berlin, Germany: Springer-Verlag, 1967.

[17] F. Holmes and P. Slade, "Suppression of pip and crater formation during interruption of alternating current circuits," *Inst. Elect. Eng. Trans. Compon. Hybrids, Manuf. Technol.*, vol. 1, no. 1, pp. 59–65, Mar. 1978.

[18] M. Weis, G. Vorlaufer, and F. Berger, "Comparison of the material transfer on corresponding electrodes in consideration of the relative position and movement of the electrical contacts," presented at the 56th IEEE Holm Conf. Elect. Contacts, Charleston, SC, Oct. 2010.

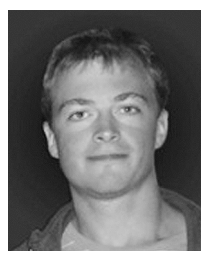

Daniel J. Rogers (M'11) received the M.Eng. and Ph.D. degrees in electrical and electronic engineering from Imperial College London, London, U.K., in 2007 and 2011, respectively.

Currently, he is a Lecturer in the Institute of Energy, Cardiff University, Cardiff, U.K. He conducts research in collaboration with industry and is involved with the development of high-performance power electronic systems for a variety of companies. He is a co-investigator on the multi-institution EPSRC Energy Storage for Low Carbon Grids project. His interests include the use of medium- and large-scale power-electronic systems to create flexible electrical networks capable of taking advantage of a diverse range of generation technologies, and the subsequent control challenges this produces.

Tim C. Green (SM'02) received the B.Sc. (Hons.) degree in electrical engineering from Imperial College, London, U.K., in 1986 and the Ph.D. degree in electrical engineering from Heriot-Watt University, Edinburgh, U.K., in 1990.

Currently, he is a Chartered Engineer in the U.K. He was a Lecturer at Heriot Watt University until 1994 and is currently a Professor of Electrical Power Engineering at Imperial College London and Deputy Head of the Electrical and Electronic Engineering Department. His research interest is in formulating the future form the electricity network to support low-carbon futures. A particular theme is how the flexibility of power electronics and control can be used to accommodate new-generation patterns and new forms of load, such as EV charging, as part of the emerging smart grid. He has particular interests in offshore dc networks and the management of low-voltage networks.

Prof. Green leads the HubNet consortium of eight U.K. universities coordinating research in low-carbon energy networks and is the Network Champion for the Research Councils U.K.